

Formation and evolution of epitaxial Co_5Ge_7 on $\text{Ge}(001)$ surface by reactive deposition inside an ultrahigh-vacuum transmission electron microscope

H. P. Sun, Y. B. Chen, and X. Q. Pan^{a)}

Department of Materials Science and Engineering, University of Michigan, Ann Arbor, Michigan 48109

D. Z. Chi, R. Nath, and Y. L. Foo

Institute of Materials Research and Engineering, 3 Research Link, Singapore 117602, Singapore

(Received 29 June 2004; accepted 9 December 2004; published online 7 February 2005)

Cobalt was deposited on single-crystal $\text{Ge}(001)$ surface at $\sim 350^\circ\text{C}$ by electron-beam evaporation in an ultrahigh-vacuum transmission electron microscope. The deposited Co reacts with Ge to form nanosized islands with the cobalt germanide Co_5Ge_7 phase. The Co_5Ge_7 islands show square and rectangular shapes. Two epitaxial orientation relationships between Co_5Ge_7 and Ge were observed: $\text{Co}_5\text{Ge}_7 \langle 110 \rangle (001) \parallel \text{Ge} \langle 100 \rangle (001)$ and $\text{Co}_5\text{Ge}_7 (001) (110) \parallel \text{Ge} \langle 100 \rangle (001)$. © 2005 American Institute of Physics. [DOI: 10.1063/1.1862331]

Ge has recently been considered as a substrate candidate by semiconductor industry to meet the sub-45 nm technology requirements due to its high carrier mobility and excellent compatibility with high- k materials. Metal germanides will be used as contact materials in the future Ge technology. Compared with silicides that have been extensively investigated in the past,¹ formation of germanides on single crystal Ge surface attracted less attention. Some earlier studies^{2,3} on cobalt germanides originated from the fact that cobalt germanides, especially CoGe_2 , can be used as contact materials in $\text{Si}_{1-x}\text{Ge}_x$ and GaAs systems. In the Co-Ge phase diagram,⁴ Co_5Ge_7 and CoGe_2 are two line compounds and are stable up to 800°C . Co_5Ge_7 is tetragonal ($a=0.76$ nm, $c=0.581$ nm) and CoGe_2 is orthorhombic ($a=b=0.5681$ nm, $c=1.0818$ nm).⁵ Solid-state reaction by thermal annealing of thin Co layer on Ge surface showed that Co_5Ge_7 will form at temperature around 300°C and then transform to CoGe_2 at temperature above 425°C .² Localized epitaxial growth of Co_5Ge_7 and CoGe_2 on single crystal $\text{Ge}(111)$ was ever observed by transmission electron microscopy (TEM).⁶ Recently, epitaxial growth of Co_5Ge_7 and CoGe_2 islands on a strained Ge epilayer on $\text{Si}(001)$ was studied by scanning tunneling microscopy (STM) and reflection high-energy electron diffraction (RHEED).⁷ In this letter, we report the formation and evolution of epitaxial Co_5Ge_7 phase on a single crystal $\text{Ge}(001)$ surface by reactive deposition in an *in situ* ultrahigh vacuum transmission electron microscope (UHV TEM).

The reactive deposition of Co on Ge was performed in a JEOL-2010 TEM that is modified for *in situ* deposition of materials under ultrahigh vacuum with a base pressure $<10^{-9}$ Torr. Electron transparent planar-view substrate was prepared by mechanical polishing and Ar^+ ion milling from the backside of a (001) oriented single crystal Ge disk. The Ge substrate was mounted on the top of a conductive silicon support to enable *in situ* heating. The substrate was then *in situ* heated to $\sim 350^\circ\text{C}$. At this temperature, residual oxygen on the surface can be completely removed, which was con-

firmed by *in situ* electron energy loss spectroscopy (EELS). Atomic Co flux was generated by electron beam evaporation of a high purity (99.998%) Co rod from an evaporator attached to the microscope. The growth rate was $\sim 0.006 \text{ \AA/s}$, calibrated by *ex situ* Rutherford backscattering (RBS) analysis.

Figure 1 displays a series of bright field TEM images taken at the different stages of the deposition of Co. Islands with appreciable size on the TEM image appeared in less than two minutes from the start of the deposition, as shown in Fig. 1(a). As deposition continues, both the size and the density of the islands increase. During growth several islands may become in contact with each other and form a larger one [Figs. 1(b) and 1(c)]. Meanwhile, new islands continue to nucleate in the open areas between the large islands, as shown in Fig. 1(d). The fine grid-like pattern appearing in the image of islands are Moiré fringes due to the overlap of the islands with Ge. Most of the islands have either square or rectangular shapes. The elongation direction or the edge of the square is parallel to one of two in-plane $\langle 110 \rangle$ directions of Ge, which was determined by selected area electron diffraction (SAED). These observations show that nanosized islands nucleate uniformly on the substrate surface. As deposition proceeds, the islands grow with well-defined faceted shapes and coalescence with each other.

SAED patterns were also obtained at different stages of the deposition corresponding to each bright field image. Electron diffraction pattern from Ge substrate before the start of the Co deposition shows a high single crystal quality. After the Co deposition proceeds, weak spots other than those of Ge gradually occur in the diffraction pattern. Figure 2(a) is a diffraction pattern taken after a deposition for 6 min. Some of the Ge diffraction spots are indexed. The intensity of those weak spots increases with the increase of the deposition time. Figure 2(b) shows a diffraction pattern after a continuing deposition for 155 min, of which the corresponding bright field image is shown in Fig. 1(d). This pattern remains unchanged even after a total 3 h deposition and cooling the sample down to room temperature.

The reflections other than that of the Ge substrate must come from either the element cobalt phase or a cobalt ger-

^{a)} Author to whom correspondence should be addressed; electronic mail: panx@umich.edu

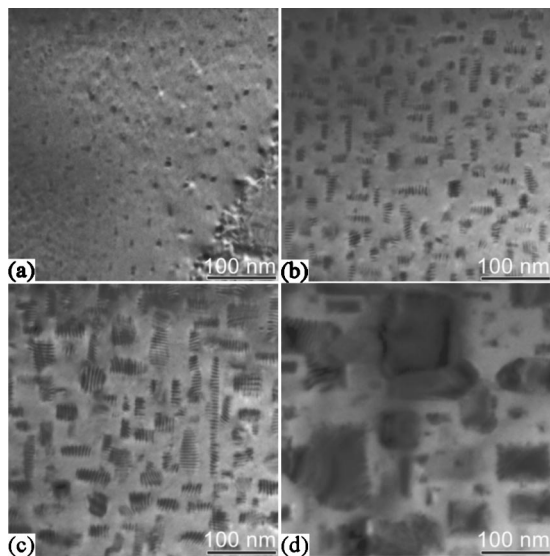


FIG. 1. Morphology evolution of Co deposited on Ge(001) surface (a) 2 min; (b) 32 min; (c) 61 min; and (d) 145 min.

manide phase as a result of reaction between Co and Ge during the deposition. Detailed analysis of the diffraction patterns shows that the observed diffraction spots cannot be indexed using any simple element Co structures including the hcp, fcc, and bcc phases.

Indeed, the observed diffraction spots in Fig. 2 can be indexed using the (001) Ge substrate and the cobalt germanide Co_5Ge_7 phase. To clearly illustrate the orientation of Co_5Ge_7 on Ge, a set of computer simulated diffraction patterns are shown in Fig. 3. Figure 3(a) is a simulated electron diffraction pattern along the Ge ($a=0.566$ nm) [001] direction. Figure 3(b) is a simulated diffraction pattern of Ge_5O_7 along the [001] direction. All diffraction spots in Figs. 2(a) and 2(b) can be obtained by overlapping Fig. 3(a) on Fig. 3(b). This indicates an epitaxial orientation with $\text{Co}_5\text{Ge}_7\langle 110\rangle(001)\parallel\text{Ge}\langle 010\rangle(001)$.

It should be pointed out that two other orientations of some Co_5Ge_7 islands, i.e., $\text{Co}_5\text{Ge}_7\langle 001\rangle(110)\parallel\text{Ge}\langle 100\rangle(001)$ may exist. Figures 3(c) and 3(d) are simulated diffraction patterns of Co_5Ge_7 along the [110] zone axis with an in-plan rotation of 90° with respect to each other. Both of these orientations are possible, given a fourfold symmetry of the Ge(001) surface. Overlapping of them on the diffraction pattern of (001) Ge will reproduce all spots, except for those occurring at the Ge $(2m+1, 2n+1, 0)$ positions in Fig. 3(b), where m and n are integers. Furthermore, the simulated diffraction pattern of CoGe_2 along the [001] zone axis will also fit the same set of diffraction spots in Fig. 2 as the two [110]

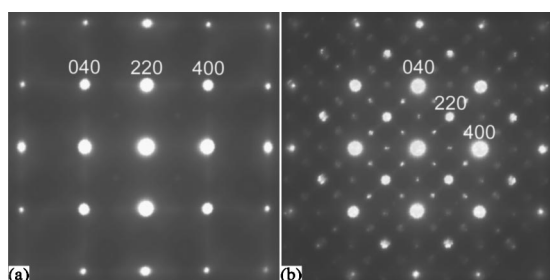


FIG. 2. Evolution of electron diffraction patterns during *in situ* deposition of Co on Ge(001), (a) 6 min and (b) 155 min.

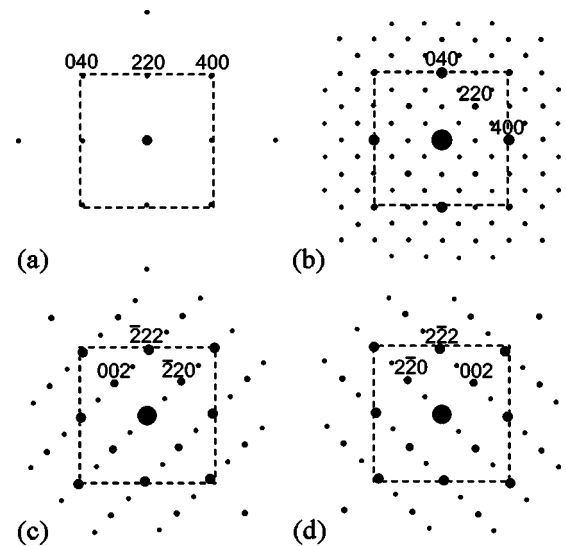


FIG. 3. Simulated electron diffraction patterns of (a) Ge[001], (b) Co_5Ge_7 [001], and (c), (d) Co_5Ge_7 [110].

Co_5Ge_7 patterns. The $\{200\}$ and $\{240\}$ reflections in the Co_5Ge_7 [001] zone-axis pattern [Fig. 3(b)] appear in Fig. 2(b), but they do not match any reflections allowed in the CoGe_2 structure. According to these studies, one can conclude the occurrence of the (001) oriented Co_5Ge_7 phase during the reactive deposition of Co on (001) Ge at 350°C . However, the existence of a small amount of the (110) oriented Ge_5O_7 and/or the (001) oriented CoGe_2 islands cannot be excluded.

X-ray diffraction (XRD) analysis was also performed on the same specimen after the *in situ* TEM studies. Except for the reflections from the (001) Ge substrate, there are only two peaks occurring in the XRD pattern. As shown in Fig. 4, the strong peak occurring at $2\theta=30.92^\circ$ results from the (002) plane (with $2\theta=30.74^\circ$) of the Co_5Ge_7 phase. However, the weak peak located at $2\theta=33.20^\circ$ may result either from the (220) plane (with $2\theta=33.14^\circ$) of Co_5Ge_7 or from the (004) plane (with $2\theta=33.11^\circ$) of the CoGe_2 phase. According to the previous studies of solid phase reaction between Co and Ge,^{2,6} Co_5Ge_7 usually form at a lower temperature around 300°C , whereas CoGe_2 occurs at a temperature higher than 425°C . Furthermore, in solid-state reaction of a thin metal film with Si, only a few phases will appear and in sequence but not simultaneously.¹ This may also be true for the reaction between metals and Ge. Thus, it is unlikely that CoGe_2 exists during the *in situ* deposition at $\sim 350^\circ\text{C}$. However, in the case of reactive deposition of metal on Si substrate, it was found that low deposition rate can reduce the effective metal concentration at the growth interface and hence reduce the substrate temperature that is required to form Si-rich silicides, usually disilicides.⁸ For example, for solid phase reaction, Co_2Si , CoSi , and CoSi_2 will appear in sequence and annealing above 550°C is required to form CoSi_2 .⁹ In contrast, it was reported that CoSi_2 forms directly on Si during a reactive deposition at 360°C with a low flux rate of 0.0008 \AA/s .¹⁰ Therefore, we cannot rule out the possibility that CoGe_2 forms during the *in situ* reactive deposition at $\sim 350^\circ\text{C}$ in the present work.

Our *in situ* experiment shows that Co_5Ge_7 is the first phase formed when Co was deposited on Ge(001) substrate at a rate of 0.006 \AA/s at $\sim 350^\circ\text{C}$. On arrival to the Ge

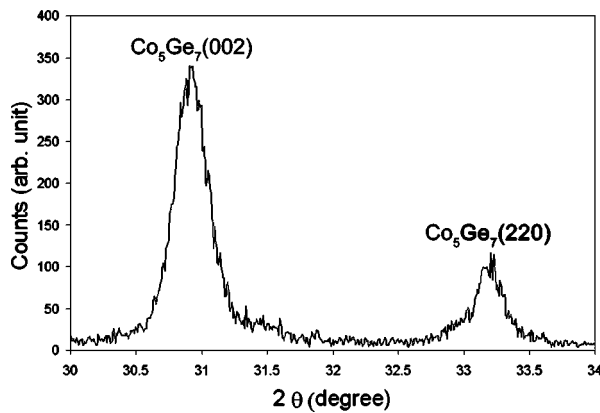


FIG. 4. XRD spectrum of the sample after the *in situ* deposition.

surface, there is an immediate incorporation of Co atoms with the Ge substrate. Diffusion of Co into Ge is required for the further growth of the Co_5Ge_7 islands. It was reported that Co atoms begin to diffuse into the bulk Ge(001) surface at a relatively low temperature ($\sim 150^\circ\text{C}$) in comparison with the diffusion of Co in Si (350°C),¹¹ hence, the formation of germanides tends to occur at temperatures lower than that for the formation of corresponding silicides.¹ For Co on Si, annealing at $550\text{--}650^\circ\text{C}$ will induce diffusion of Co into the Si lattice with Co atoms staying in the interstitial sites only.¹² This may also be true for Co on Ge considering that both Ge ($a=0.566\text{ nm}$) and Si ($a=0.543\text{ nm}$) have diamond structure. Initially there might be a random occupation of the Co in the interstitial sites near the surface region of the Ge substrate. With continued deposition and incorporation of Co atoms into the lattice, at a certain point, nucleation and formation of the Co_5Ge_7 islands is thermodynamically favorable.

No metallic hcp-Co is likely to nucleate on the Ge surface when the deposition rate of Co is small in comparison with the reaction rate of the Co atoms with the substrate. The reaction rate is controlled by the substrate temperature. Once the Co_5Ge_7 phase formed, it will block the immediate interaction between the Co flux and underlying Ge. Arriving Co atoms may reach the $\text{Co}_5\text{Ge}_7/\text{Ge}$ interface by diffusion through the Co_5Ge_7 layer and/or the Ge surface between Co_5Ge_7 islands. Interstitial Co atoms can also diffuse through the host Ge lattice to reach to the $\text{Co}_5\text{Ge}_7/\text{Ge}$ interface.

Because the Co_5Ge_7 islands are partially embedded in the Ge matrix, they will experience an in-plane tensile or compression stress from the Ge matrix depending on the sign of lattice mismatch. For the epitaxial growth of Co_5Ge_7 on (001) Ge with the orientation relationship of $\text{Co}_5\text{Ge}_7[001](110)\parallel\text{Ge}[100](001)$, there will be 2.3% lattice misfit along the [001] direction of Co_5Ge_7 (compression stress) and -4.5% along the perpendicular $\langle\bar{1}10\rangle$ direction (tensile stress). Such an anisotropic stress can lead to an elongation of the island. However, the population of islands with this orientation is small according to TEM observations. The majority of Co_5Ge_7 islands have the orientation relationship of $\text{Co}_5\text{Ge}_7(110)(001)\parallel\text{Ge}(010)(001)$. There will be -4.5% mismatch strain along the [100] and [010] directions of Co_5Ge_7 and the islands are under a tensile stress.

For these islands, the strain relaxation and minimization of interfacial energy can also cause an elongation of the islands along either the [100] or [010] direction of the Co_5Ge_7 islands. As shown in Figs. 1(b) and 1(c), the Moiré fringes appear along the direction perpendicular to the elongation of the islands. This reveals that the lattice misfit strain in the elongated Co_5Ge_7 islands is relaxed along the elongation direction and that the Co_5Ge_7 islands have coherent interfaces with the Ge substrate along the perpendicular direction.

If the strain relaxation occurs along both the [100] and [010] directions, the Co_5Ge_7 island will grow uniformly along the both directions and a squared shape of the islands will form. For such islands, Moiré fringes appear along both [100] and [010] directions, as shown in Fig. 1(c). This usually occurs when the thickness of islands exceeds a critical value.

According to the XRD analysis, the misfit strain is not completely relaxed. Figure 3 shows that the (002) peak of Co_5Ge_7 is shifted from 30.74° for a bulk crystal to 30.92° in the *in situ* reacted film, which is corresponding to a decrease of the lattice parameter c from 0.581 nm for bulk to 0.578 nm for the strained film. In Fig. 3, the (220) peak of Co_5Ge_7 is shifted from 30.14° for a bulk crystal to 30.20° in the *in situ* reacted film indicating a slight decrease of the lattice spacing of the $\text{Co}_5\text{Ge}_7(110)$ plane from 0.2701 nm (in bulk) to 0.2696 nm .

In conclusion, epitaxial Co_5Ge_7 islands were observed in the reactive deposition of Co on the (001) Ge surface at $\sim 350^\circ\text{C}$ using an *in situ* UHV TEM. Two epitaxial orientation relationships between Co_5Ge_7 and Ge were observed: $\text{Co}_5\text{Ge}_7(001)(110)\parallel\text{Ge}(100)(001)$ (majority) and $\text{Co}_5\text{Ge}_7(110)(001)\parallel\text{Ge}(100)(001)$ (minority). The Co_5Ge_7 islands show square or rectangular shapes.

This work was supported partially by the Institute of Materials Research and Engineering (IMRE) in Singapore and by the National Science Foundation (NSF) through Grant No. NSF/DMR 0308012. The authors would like to thank Chi-Wen Soo, Dr. Shi-Jie Wang, and Professor Alfred Huan for their kind support during the *in situ* deposition experiment at IMRE.

¹S. L. Zhang and M. Ostling, *Crit. Rev. Solid State Mater. Sci.* **28**, 1 (2003).

²S. P. Ashburn, M. C. Ozturk, G. Harris, and D. M. Maher, *J. Appl. Phys.* **74**, 4455 (1993).

³K. E. Mello, S. P. Murarka, T.-M. Lu, and S. L. Lee, *J. Appl. Phys.* **81**, 7261 (1997).

⁴T. B. Massalski, *Binary Alloy Phase Diagrams* (American Society for Metals, Metals Park, OH, 1986).

⁵W. B. Pearson, *Pearson's Handbook of Crystallographic Data for Intermetallic Phases* (American Society for Metals, Metals Park, OH, 1985), p. 1770.

⁶Y. F. Hsieh, L. J. Chen, E. D. Marshall, and S. S. Lau, *Appl. Phys. Lett.* **51**, 1588 (1987).

⁷I. Goldfarb and G. A. D. Briggs, *J. Mater. Res.* **16**, 744 (2001).

⁸A. Vantomme, S. Degroote, J. Dekoster, G. Langouche, and R. Pretorius, *Appl. Phys. Lett.* **74**, 3137 (1999).

⁹M.-A. Nicolet and S. S. Lau, in *VLSI Electronics: Microstructure Science*, edited by N. G. Einspruch and G. B. Larrabee (Academic, New York, 1983), Vol. 6, Chap. 6.

¹⁰L. Haderbache, P. Wetzel, C. Pirri, J. C. Peruchetti, D. Bolmont, and G. Gewinner, *Appl. Phys. Lett.* **53**, 1384 (1988).

¹¹K. Prabhakaran and T. Ogino, *Appl. Surf. Sci.* **100/101**, 518 (1996).

¹²H. L. Meyerheim, U. Döbler, and A. Puschmann, *Phys. Rev. B* **44**, 5738 (1991).